Collective Modes in Strongly Correlated Yukawa Liquids: Waves in Dusty Plasmas

G. Kalman,[1] M. Rosenberg,[2] and H. E. DeWitt[3]

[1]*Department of Physics, Boston College, Chestnut Hill, Massachusetts 02467*

[2]*Department of Electrical and Computer Engineering, University of California, San Diego, La Jolla, California 92093*

[3]*Lawrence Livermore National Laboratory, Livermore, California 94550*

(Received 23 December 1999)

We determine the collective mode structure of a strongly correlated Yukawa fluid, with the purpose of analyzing wave propagation in a strongly coupled dusty plasma. We identify a longitudinal plasmon and a transverse shear mode. The dispersion is characterized by a low-k acoustic behavior, a frequency maximum well below the plasma frequency, and a high-k merging of the two modes around the Einstein frequency of localized oscillations. The damping effect of collisions between neutrals and dust grains is estimated.

PACS numbers: 52.25.Ub, 52.25.Zb, 52.35.Fp, 52.35.Lv

The feasibility of creating strongly coupled dusty plasmas in the laboratory is by now solidly established [1]. For low frequency processes the dynamical system in the dusty plasmas consists only of the massive grains that carry extremely high ($Z = 10^3 \sim 10^4$) negative charges. The role of the electrons and to some extent of the ions is reduced to providing a polarizable background. While in laboratory dusty plasmas the ions may possess a directed velocity, induced by the electric field which is created to levitate the system, for the purpose of the discussion in the paper the streaming velocity of the ions is largely ignored. Thus the interaction between the dust grains is fairly well described through a linearized Debye screened potential. If ions and electrons are treated on the same footing, the screening length λ_D is given by $\lambda_D = (\lambda_{De}^{-2} + \lambda_{Di}^{-2})^{-1/2}$, but it has been argued that in view of the nonequilibrium behavior of the ions $\lambda_D = \lambda_{De}$ is a better choice (λ_D is the Debye radius). With this modeling, the dusty plasma is a good realization of a one-component strongly coupled Yukawa system with interaction potential $\Phi(r) = \frac{Z^2e^2}{r} e^{-\kappa r}$, $\kappa = \lambda_D{}^{-1}$. A Yukawa system is characterized by two parameters, $\Gamma = \frac{Z^2e^2}{k_BTa}$ and $\overline{\kappa} = \kappa a$, a being the Wigner-Seitz radius, $\frac{4\pi}{3} na^3 = 1$. While in the one component plasma (OCP) Γ is a good measure of the interparticle coupling, here, because of the screening, it is not. Instead, the combination $\Gamma_{\rm eff} = \Gamma e^{-\overline{\kappa}}$ can be used. In a strongly coupled dusty plasma $\Gamma_{\rm eff}$ and *a fortiori* Γ have high values and the system is either in the liquid or in the crystalline solid state. The phase diagram has recently been given by [2]. As to the collective mode structure in the liquid and solid phases, one expects to find a longitudinal and a transverse mode similarly to the OCP [3–6], with the important difference that the longitudinal mode would also acquire an acoustic dispersion. Recent molecular dynamics simulation work [7] corroborates this picture and portrays the mode structure for a wide range of Γ and $\overline{\kappa}$ values. On the theoretical side, however, apart from a few attempts, mostly concentrating on the low-k domain [8–10], a comprehensive description and understanding of the mode structure has been lacking. In this Letter, we report on the results of a consistent theoretical analysis of the collective mode structure of a Yukawa system in the strongly coupled liquid phase. The analysis is based on the quasilocalized charge approximation (QLCA), which has a proven record of successfully describing collective behavior in a series of strongly coupled plasma systems [3,11,12]. The QLCA is founded on the physical model that suggests that for a substantial portion of their time history particles in a strongly interacting system are trapped and oscillate in the momentary local minima of the fluctuating potential. While the present study is motivated by the dusty plasma problem, our analysis is directed at the properties of an idealized Yukawa fluid: some differences between this latter and actual laboratory dusty plasmas will be pointed out at the end of this Letter.

All the information pertinent to the dynamics of the system is included in the dielectric tensor $\varepsilon(\mathbf{k}\omega)$ which can be decomposed into longitudinal (L) and transverse (T) parts:

$$\varepsilon(\mathbf{k}\omega) = \varepsilon_L(\mathbf{k}\omega)\frac{\mathbf{k}\mathbf{k}}{k^2} + \varepsilon_T(\mathbf{k}\omega)\left(1 - \frac{\mathbf{k}\mathbf{k}}{k^2}\right). \tag{1}$$

The QLCA calculations for the longitudinal and the transverse dielectric functions provide

$$\varepsilon_{L/T}(\mathbf{k}\omega) = 1 - \frac{\omega_0^2(\mathbf{k})}{\omega^2 - D_{L/T}(\mathbf{k})}, \tag{2}$$

where the $D_L(\mathbf{k})$ and $D_T(\mathbf{k})$ local field functions are respective projections of the QLCA dynamical matrix $D_{\mu\nu}(\mathbf{k})$ [11]. They are functionals of the equilibrium pair correlation function $g(\mathbf{r})$ or of its Fourier transform $g(\mathbf{k})$; $\omega_0(\mathbf{k})$ is the frequency of the longitudinal-acoustic wave in the random phase (Vlasov) approximation:

$$\omega_0^2(\mathbf{k}) = \frac{n}{m}\phi(\mathbf{k})k^2 = \omega_p^2\frac{k^2}{k^2 + \kappa^2}, \tag{3}$$

with

$$\omega_p = \left(\frac{4\pi e^2Z^2n}{m}\right)^{1/2} \quad \text{and} \quad \phi(\mathbf{k}) = \frac{Z^2e^2}{k^2 + \kappa^2}. \tag{4}$$

 0031-9007/00/84(26)/6030(4)$15.00

The collective excitations are governed by the dispersion relations

$$\varepsilon_L(\mathbf{k}\omega) = 0, \tag{5}$$

$$\varepsilon_T^{-1}(\mathbf{k}\omega) = 0 \tag{6}$$

that describe a longitudinal and a transverse mode:

$$\omega_L(\mathbf{k}) = \sqrt{\omega_0^2(\mathbf{k}) + D_L(\mathbf{k})}, \tag{7}$$

$$\omega_T(\mathbf{k}) = \sqrt{D_T(\mathbf{k})}. \tag{8}$$

The original development of the QLCA [11] was directed at applications to systems with long range Coulomb interaction. The algorithm is, however, easily generalized to an arbitrary interaction potential (see also [13]); this calculation yields the dynamical matrix $D_{\mu\nu}(\mathbf{k})$, expressed in terms of $g(\mathbf{r})$:

$$D_{\mu\nu}(\mathbf{k}) = \frac{n}{m}\int d^3r\, M_{\mu\nu}(\mathbf{r})\,(e^{i\mathbf{k}\cdot\mathbf{r}} - 1)g(\mathbf{r}). \tag{9}$$

$M_{\mu\nu}(\mathbf{r})$ is the dipole-dipole interaction potential associated with $\phi(\mathbf{r})$

$$M_{\mu\nu}(\mathbf{r}) = -\frac{4\pi Z^2 e^2}{r^3}\, e^{-\kappa r}\left\{\delta_{\mu\nu}(1 + \kappa r) - 3\,\frac{r_\mu r_\nu}{r^2} \times \left(1 + \kappa r + \frac{1}{3}\,\kappa^2 r^2\right)\right\}. \tag{10}$$

The local fields are now expressed through the relations $D_L(\mathbf{k}) = \frac{k_\mu k_\nu}{k^2}\, D_{\mu\nu}(\mathbf{k})$, $D_T(\mathbf{k}) = \frac{1}{2}\,[D_0(\mathbf{k}) - D_L(\mathbf{k})]$ and $D_0(\mathbf{k}) = D_{\mu\mu}(\mathbf{k})$ which lead to the explicit results

$$D_{0,L}(\mathbf{k}) = \omega_p^2 \int d\bar{r}\, \frac{e^{-\bar{\kappa}\bar{r}}}{\bar{r}}\, \mathcal{D}_{0,L}(\bar{r},\bar{k})g(\bar{\mathbf{r}}), \tag{11}$$

with

$$\mathcal{D}_0(\bar{r},\bar{k}) = \bar{\kappa}^2\bar{r}^2\left(1 - \frac{\sin\bar{\kappa}\,\bar{r}}{\bar{k}\bar{r}}\right) \tag{12}$$

and

$$\mathcal{D}_L(\bar{r},\bar{k}) = -2\left\{[(1 + \bar{\kappa}\,\bar{r}) + (\bar{\kappa}\,\bar{r})^2]\left(\frac{\sin\bar{\kappa}\,\bar{r}}{\bar{k}\bar{r}} + 3\,\frac{\cos\bar{\kappa}\,\bar{r}}{(\bar{k}\bar{r})^2} - 3\,\frac{\sin\bar{\kappa}\,\bar{r}}{(\bar{k}\bar{r})^3}\right) - \frac{1}{6}\,(\bar{\kappa}\,\bar{r})^2\left(1 + 3\,\frac{\sin\bar{\kappa}\,\bar{r}}{\bar{k}\bar{r}} + 12\,\frac{\cos\bar{\kappa}\,\bar{r}}{(\bar{k}\bar{r})^2} - 12\,\frac{\sin\bar{\kappa}\,\bar{r}}{(\bar{k}\bar{r})^3}\right)\right\}. \tag{13}$$

The barred notation indicates dimensionless variables: $\bar{r} = r/a$, $\bar{k} = ka$, etc.

Both the longitudinal and transverse waves exhibit *acoustic* behavior in the sense that

$$\omega_{L,T}(\mathbf{k}) = s_{L,T}\,k \tag{14}$$

for $k \to 0$. The longitudinal and transverse phase velocities s_L and s_T are given by

$$s_L^2 = \frac{+2}{15}\,\omega_p^2 \int d\bar{r}\;\bar{r}g(\bar{r})e^{-\bar{\kappa}\bar{r}}\left\{1 + \bar{\kappa}\,\bar{r} + \frac{3}{4}\,(\bar{\kappa}\,\bar{r})^2\right\}a^2 + \frac{\omega_p^2 a^2}{\bar{\kappa}^2}, \tag{15}$$

$$s_T^2 = \frac{-1}{15}\,\omega_p^2 \int d\bar{r}\;\bar{r}g(\bar{r})e^{-\bar{\kappa}\bar{r}}\left\{1 + \bar{\kappa}\,\bar{r} - \frac{1}{2}\,(\bar{\kappa}\,\bar{r})^2\right\}a^2. \tag{16}$$

For $\bar{k} \ll 1$, Eqs. (15) and (16) can be related to the energy integral

$$\mathcal{E}_c(\bar{\kappa}) = \frac{1}{2}\,\frac{\beta n}{\Gamma}\int d^3r\,\phi(\mathbf{r})g(\mathbf{r}) = \frac{3}{2}\int d\bar{r}\;\bar{r}e^{-\bar{\kappa}\bar{r}}g(\bar{r}), \tag{17}$$

where $\mathcal{E}_c = \beta E_c/\Gamma$, E_c being the correlation energy, whose precise significance is that, in general, the total interaction energy $E_{\rm int}$ comprises the positive Hartree, the negative correlation, and the negative binding energy contributions [8,14] $E_{\rm int} = E_H + E_c + E_b$, $E_H = \frac{3}{2\bar{\kappa}^2}$, $E_b = -\bar{\kappa}/2$. In the present context, however, only E_c is of relevance. One can demonstrate [15] that for $\bar{\kappa} < 2$ the $\bar{\kappa}$ dependence of $g(r;\bar{\kappa})$ is quite weak and can be ignored: thus, in calculating $\mathcal{E}_c(\bar{\kappa})$ one can assume that all the $\bar{\kappa}$ dependence coming from the integrals in Eqs. (15)–(17) originates from the kernels only. As a result, (15) and (16) become functionals of $\mathcal{E}_c(\bar{\kappa})$, resulting in Eqs. (19)–(21) below.

In the $k \to \infty$ limit, both the longitudinal and transverse mode frequencies approach the common limit, $\omega *$, the Einstein frequency which is the oscillation frequency of a single particle in the fixed environment of the average background of the other particles. Letting $k \to \infty$ in (12) or in (13), one finds

$$\omega_* = \frac{\omega_p}{\sqrt{3}}\left\{1 + \frac{2}{3}\,\bar{\kappa}^2\mathcal{E}_c\right\}^{1/2}. \tag{18}$$

Evidently, ω_* is always below the corresponding OCP value [3] $(\omega_p/\sqrt{3})$. As it is easily shown, for $\bar{\kappa} \to \infty$, $\mathcal{E}_c \to -\frac{3}{2\bar{\kappa}^2}$, the negative of the Hartree energy; thus ω_* vanishes faster than $\bar{\kappa}^{-2}$ in the same limit. This is illustrated in the inset of Fig. 1.

The expressions (15) and (16) obtained for s_L and s_T and more generally for the dispersion relations (7), (8), (11)–(13) are functions of the pair correlation function $g(\mathbf{r})$. By following the hypernetted chain (HNC) scheme [16] for the computation, we have recently computed $g(\mathbf{r})$ for a Yukawa system within a wide range of Γ and $\bar{\kappa}$ values. The details of this work will be given in a separate publication (see also [15]). We have compared the energy values calculated with the aid of $g(\mathbf{r})$ with those given by [2]: the agreement was found to be very good. Thus

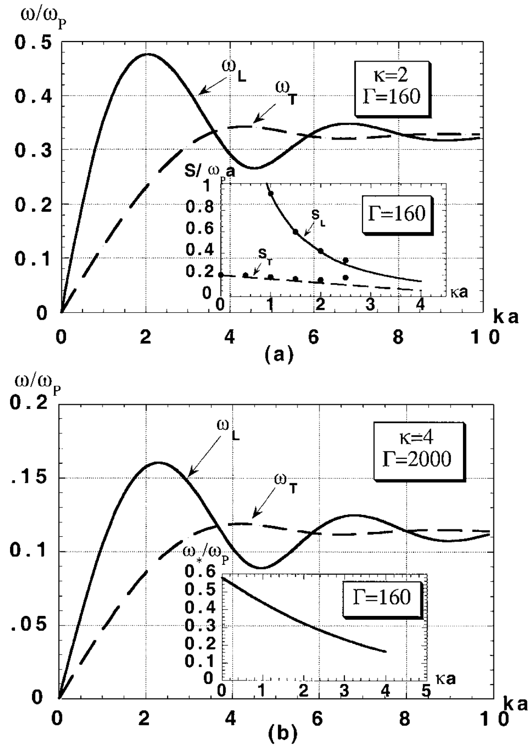

FIG. 1. Longitudinal (plasmon) and transverse (shear) mode dispersions. The inset in (a) shows the longitudinal and transverse acoustic phase velocities: The points marked (•) are the results of the approximate formulas (19)–(21). The inset in (b) shows the Einstein frequency $\omega_* \equiv \omega(k \to \infty)$, which is approximately equal to the frequency where the two modes intersect.

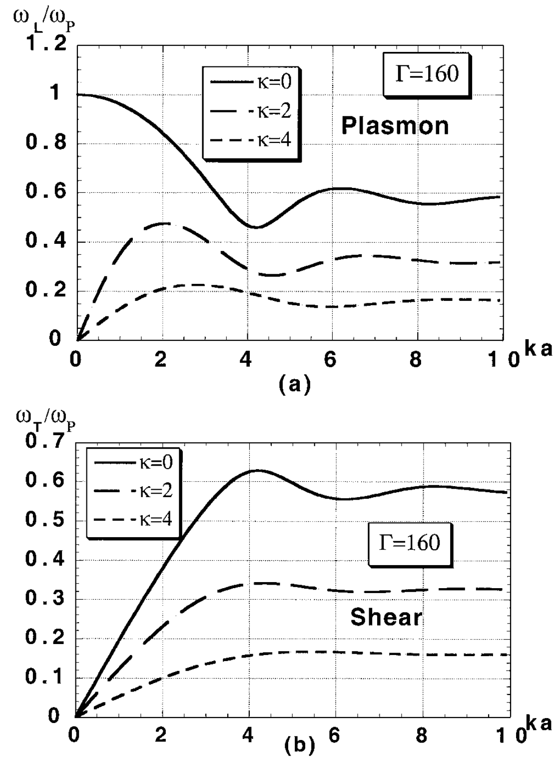

FIG. 2. The plasmon mode (a) and the shear mode (b) for different κ values.

we can use the fitting formula given by [14] valid for $\overline{\kappa} < 2.5$, to obtain an analytic expression for $\mathcal{E}_c(\overline{\kappa})$ and for its derivatives (as it was done in [8]) in order to obtain an approximate expression for the phase velocities:

$$\begin{aligned} s_L{}^2 &= \omega_p^2 a^2 \left\{ \frac{1}{\overline{\kappa}^2} + f(\overline{\kappa}) \right\}, \\ s_T{}^2 &= \omega_p^2 a^2 h(\overline{\kappa}). \end{aligned} \tag{19}$$

To leading order in Γ

$$f(\overline{\kappa}) = -0.0799 - 0.0046\overline{\kappa}^2 + 0.0016\overline{\kappa}^4, \tag{20}$$

$$h(\overline{\kappa}) = +0.0399 - 0.0090\overline{\kappa}^2 + 0.0012\overline{\kappa}^4. \tag{21}$$

The inset in Fig. 2 shows the variation of the longitudinal and transverse phase velocities with $\overline{\kappa}$ both as given by Eqs. (19)–(21), and as calculated directly from the more exact relations, Eqs. (15) and (16). The longitudinal velocity, as discussed in [8], decreases with increasing $\overline{\kappa}$; the transverse shear velocity shows a slower decrease, and for $\overline{\kappa} > 5$ they approach each other closely.

The full $\omega(\mathbf{k})$ dispersion curves for different Γ and $\overline{\kappa}$ values portrayed in Figs. 1 and 2. All the $\Gamma - \kappa$ contributions chosen in Figs. 1–3 lie below the liquid-solid phase boundary of Ref. [2]. The main features of the mode dispersions, in addition to those discussed above, are as follows: (i) The plasmon mode reaches a maximum frequency $\omega_{\max}$ (around $\overline{k}_{\max} = 2–3$) which is below the plasma frequency ω_p; $\omega_{\max}$ drops dramatically with increasing $\overline{\kappa}$ values. (ii) As the plasmon frequency drops after its maximum and the shear frequency keeps increasing, the two dispersion curves intersect each other at around $\overline{k}_{\text{int}} = 3–6$, providing a common frequency ω_{int}, in the vicinity of ω_*, the asymptotic Einstein frequency. (iii) The first intersection is followed by a series of damped oscillations, and a characteristic braided structure of the plasmon and shear waves: this behavior is the reflection of the incipient Brillouin zones induced by the short range order.

Our results, based on the theoretical model, have been compared with recent MD simulation data by Ohta and Hamaguchi [7]. The comparison for a selected set of $\overline{\kappa}$ and Γ values is shown in the inset in Fig. 3. The agreement is very good, except for the transverse mode which vanishes for small wave numbers since in the liquid phase shear cannot be maintained for $k \to 0$. Because of the diffusive migration of particles, which is slow, but not negligible on a long time scale, failure of the QLCA in the low frequency (long time) limit is not unexpected and is explained in more detail elsewhere [3,17].

The QLCA is not geared to describe the damping of modes, but similarly to what has been done for other systems [11,15,17] an estimate can be made based on the diffusion of the particles from their quasilocalized position. In a dusty plasma environment, however, a more important limitation on the wave propagation is set by the dust-neutral collisions.

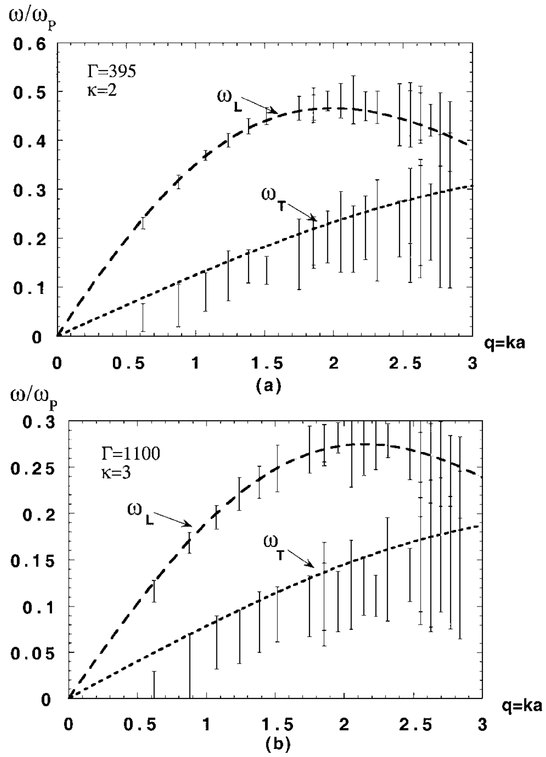

FIG. 3. Comparison of the results of this work with the MD data of Ref. [7].

The hard-sphere dust neutral collision frequency is given by $\nu_{dn} \approx \pi R^2 n_n V_n m_n / m$ (R, m are the radius and mass of the dust grains, and n_n, V_n, and m_n are the density, thermal speed, and mass of the neutrals). Using some nominal parameters of strongly coupled dusty plasma experiments (e.g., [1]), namely, $n_n \approx 10^{16}$ cm^{-3} (for $\frac{1}{2}$ mbar Ar at room temperature), $R = 4\ \mu$m, $n \approx 3 \times 10^4$ cm^{-3}, and estimating $Z \approx 10^4$ (using $T_e \approx 2$ eV) and $m \approx 2 \times 10^{14}\ m_p$ (assuming dust mass density $\rho \approx 1.5$ g/cm^3), yields the estimate $\nu_{dn}/\omega_p \approx \frac{1}{4}$. Collisional effects would be expected to dominate for $k \to 0$ since both ω_L and ω_T are $\ll \omega_p$ in this wavelength regime [3,17]. The effect of dust-neutral collisions on the longitudinal mode has been discussed in [8]. For small (but finite) k, dust-neutral collisions are important for the shear mode when $\nu_{dn} > \omega_T \approx \omega_p ka \sqrt{h(\overline{\kappa})}$, where $h(\overline{\kappa})$ is given by Eq. (21) for large Γ and $\overline{\kappa} \leq 1$. For example, for $ka = 0.5$ and $\overline{\kappa} = 1$, collisions dominate when $\nu_{dn}/\omega_p > 0.09$. Since this value is smaller than the estimate given above, the ratio ν_{dn}/ω_p would have to be reduced experimentally in order to observe the wave. The collision rate $\nu_{dn} \propto R^2 m_n^{1/2}/m$ (keeping n_n fixed), while $\omega_p \propto (Z^2/m)^{1/2}$. Since $Z \propto R$, while $m \propto \rho R^3$, the ratio $\nu_{dn}/\omega_p \propto (m_n/R\rho)^{1/2}$. Thus, we propose that experiments use a lighter gas and a dust material with larger specific gravity to reduce collisional effects. For example, using He gas and gold dust particles would reduce ν_{dn}/ω_p estimated above by a factor of about 10 (i.e., $\nu_{dn}/\omega_p \approx 0.025$), in which case both the transverse mode and strong coupling effects on the longitudinal mode might be observed.

The work of G. K. and M. R. was partially supported by Grants No. DE-FG02-98ER54501 (G. K.) and No. DE-FG03-97ER54444 (M. R. and G. K.); the work of HEDW was performed under the auspices of the U.S. Department of Energy under Contract No. W-7405-Eng-48 for the Lawrence Livermore National Laboratory. G. K. wishes to acknowledge useful conversations with Kenneth I. Golden. We thank S. Hamaguchi for making his data available to us prior to publication. We thank Tom Sullivan for computational help.

[1] H. Thomas, G. E. Morfill, V. Demmel, J. Goree, B. Feuerbacher, and D. Mohlmann, Phys. Rev. Lett. **73**, 652 (1994); J. H. Chu and Lin I, Physica (Amsterdam) **205A**, 183 (1994); J. H. Chu and Lin I, Phys. Rev. Lett. **72**, 4009 (1994); Y. Hayashi and K. Tachibana, Jpn. J. Appl. Phys. **33**, L804 (1994); A. Melzer, T. Trottenberg, and A. Piel, Phys. Lett. A **191**, 301 (1994); J. B. Pieper and J. Goree, Phys. Rev. Lett. **77**, 3137 (1996).

[2] S. Hamaguchi, R. T. Farouki, and D. H. E. Dubin, J. Chem. Phys. **105**, 7641 (1996); Phys. Rev. E **56**, 4671 (1997).

[3] (a) K. I. Golden, G. Kalman, and Ph. Wyns, Phys. Rev. A **46**, 3454 (1992); (b) **46**, 3463 (1992).

[4] K. I. Golden, G. Kalman, L. Miao, and R. R. Snapp, Phys. Rev. B **55**, 16 349 (1997).

[5] J. P. Hansen, I. R. McDonald, and E. L. Pollock, Phys. Rev. A **11**, 1025 (1975).

[6] P. Schmidt, G. Zwicknagel, P.-G. Reinhard, and C. Toepffer, Phys. Rev. E **56**, 7310 (1997).

[7] S. Hamaguchi, in *Proceedings of the International Conference on Strongly Coupled Coulomb Systems, St. Malo, France, 1999* [J. Phys. (Paris) IV **10**, (1999)]; H. Ohta and S. Hamaguchi, Phys. Rev. Lett. **84**, 6026 (2000).

[8] M. Rosenberg and G. Kalman, Phys. Rev. E **56**, 7166 (1997).

[9] M. Murillo, in *Proceedings of the International Conference on Strongly Coupled Coulomb Systems, St. Malo, France, 1999* [J. Phys. (Paris) IV **10**, (1999)].

[10] P. K. Kaw and A. Sen, Phys. Plasmas **5**, 3552 (1998).

[11] G. Kalman and K. I. Golden, Phys. Rev. A **41**, 5516 (1990).

[12] K. Golden, Phys. Rev. A **35**, 5278 (1987).

[13] G. Kalman and K. I. Golden, in *Condensed Matter Theories*, edited by L. Blum and B. S. Malik (Plenum Press, New York, 1993).

[14] S. Hamaguchi and R. T. Farouki, J. Chem. Phys. **101**, 9876 (1994); R. T. Farouki and S. Hamaguchi, *ibid.* **101**, 9885 (1994).

[15] G. Kalman, M. Rosenberg, and H. E. DeWitt, in *Proceedings of the International Conference on Strongly Coupled Coulomb Systems, St. Malo, France, 1999* [J. Phys. (Paris) IV **10**, (1999)].

[16] W. L. Slattery, G. D. Doolen, and H. E. DeWitt, Phys. Rev. A **21**, 2087 (1980); **26**, 2255 (1982).

[17] G. Kalman, V. Valtchinov, and K. I. Golden, Phys. Rev. Lett. **82**, 3124 (1999).